

Structure–Activity Relationships

Aggregation-Induced Emission Rotors: Rational Design and Tunable Stimuli Response

Jie Li,^[a] Yang Zhang,^[b] Ju Mei,^[a] Jacky W. Y. Lam,^[a] Jianhua Hao,^[b] and Ben Zhong Tang^{*[a, c, d]}

Abstract: A novel molecular design strategy is provided to rationally tune the stimuli response of luminescent materials with aggregation-induced emission (AIE) characteristics. A series of new AIE-active molecules (AIE rotors) are prepared by covalently linking different numbers of tetraphenylethene moieties together. Upon gradually increasing the number of rotatable phenyl rings, the sensitivity of the response of the AIE rotors to viscosity and temperature is significantly enhanced. Although the molecular size is further enlarged,

the performance is only slightly improved due to slightly increased effective rotors, but with largely increased rotational barriers. Such molecular engineering and experimental results offer more in-depth insight into the AIE mechanism, namely, restriction of intramolecular rotations. Notably, through this rational design, the AIE rotor with the largest molecular size turns out to be the most viscosensitive luminogen with a viscosity factor of up to 0.98.

Introduction

Stimuli-responsive luminescent materials are of great interest either in academic research or for practical applications. Numerous studies have been conducted to develop varieties of stimuli-responsive fluorescent systems, such as pH indicators,^[1] temperature monitors,^[2,8a,9a,10] pressure sensors,^[3] viscosity probes,^[4] mechanochromic materials,^[5] and light switches,^[6,9b] mainly to extensively explore their functions and mechanisms. Meanwhile, the sensitivity and tunability of the response is also crucial to achieve good performance of stimuli-responsive materials. Therefore, molecular design strategies to regulate the sensitivity should also be established to acquire tunable stimuli responses and satisfy different requirements for various applications; however, these are rarely investigated.^[7]

By taking excimer/exciplex formation,^[8] Förster resonance energy transfer (FRET),^[2b,9] charge transfer,^[10] excited-state intramolecular proton transfer (ESIPT),^[11] and so forth as the working principles, many stimuli-responsive luminescent systems have been designed with conventional chromophores as their signal reporters; however, these normally encounter the aggregation-caused quenching (ACQ) effect.^[12] On the contrary, luminescent materials with aggregation-induced emission (AIE) characteristics, after more than 10 years of development,^[13] have also been widely explored for the response of different smart systems to pH,^[14,15a] temperature,^[15,17] viscosity,^[16] pressure, mechanical force,^[17] and so forth. Their working strategy is mainly based on the restriction of intramolecular rotations (RIR), which was proposed and extensively verified as the major mechanism for the AIE phenomenon.^[13] From the viewpoint of materials, AIE-active materials open up a new materials 'magic box' for versatile and sensitive stimuli-responsive systems, whereas from the viewpoint of the mechanism, RIR can serve as a simple and effective design principle.

However, to date, the sensitivity and tunability of the stimuli response of AIE-active smart materials has rarely been investigated. To molecularly manipulate the stimuli response of AIE materials, we should go deeper into the RIR mechanism. Such factors as the number of rotors, freedom of rotors, molecular size, electronic conjugation, conformational crowdedness, and so forth should affect the intramolecular rotations of AIE-active materials, and their effect on the RIR process thus needs to be studied in detail through appropriate molecular engineering. Although some smart molecular designs, including conformational chemical locking^[18b,c,e] and steric restrictions,^[18a,d] have been conducted to directly regulate the AIE behavior and verify the RIR mechanism, there is still a lack of a systematic understanding of AIE-active materials with a tunable stimuli response and molecular design principles.

[a] Dr. J. Li, Dr. J. Mei, Dr. J. W. Y. Lam, Prof. B. Z. Tang
Department of Chemistry, Institute for Advanced Study
Institute of Molecular Functional Materials
Division of Biomedical Engineering
The Hong Kong University of Science and Technology (HKUST)
Clear Water Bay, Kowloon, Hong Kong (S.A.R. China)
E-mail: tangbenz@ust.hk

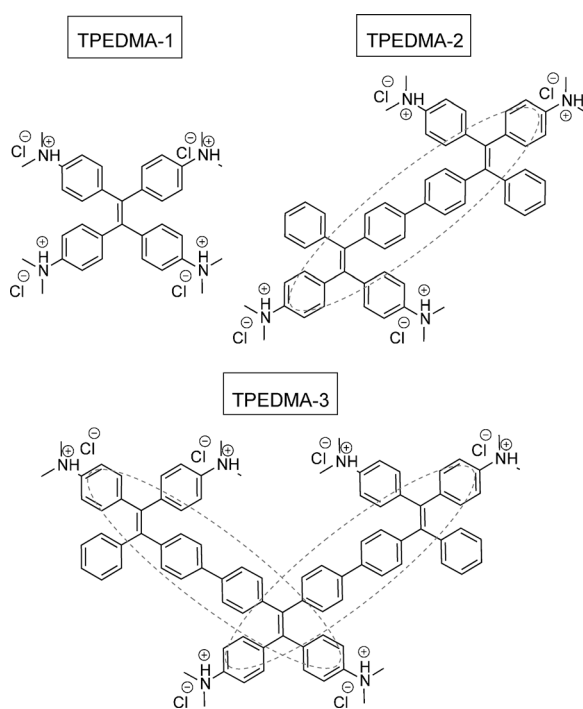
[b] Dr. Y. Zhang, Prof. J. Hao
Department of Applied Physics
The Hong Kong Polytechnic University
Hong Kong, Hong Kong (S.A.R. China)

[c] Prof. B. Z. Tang
Center for Display Research
State Key Laboratory of Luminescent Materials and Devices
South China University of Technology
Guangzhou 510640 (P.R. China)

[d] Prof. B. Z. Tang
HKUST Shenzhen Research Institute
Nanshan, Shenzhen 518057 (P.R. China)

Supporting information for this article is available on the WWW under <http://dx.doi.org/10.1002/chem.201405118>.

Herein, we report on such a novel molecular design, wherein a series of molecules with different numbers of tetraphenylethene (TPE), which is an archetypical AIE-active molecule, are chemically linked together to form AIE rotors. Upon increasing the number of rotors and enlarging the molecular size, TPEDMA-2 exhibits much higher sensitivity response to either viscosity or temperature than that of TPEDMA-1. Upon adding one more TPE moiety (TPEDMA-3), the sensitivity is only slightly improved. The chromophore with currently the highest viscosity sensitivity was developed with the guidance of this molecular design principle.



Results and Discussion

Molecular design and synthesis

Chart S1 in the Supporting Information shows the synthetic routes to TPEDMA-1, TPEDMA-2, and TPEDMA-3. These compounds were prepared through protonation of their precursors, *p*-TPEDMA-1, *p*-TPEDMA-2, and *p*-TPEDMA-3, respectively, wherein the ammonium salt was designed to provide good solubility in polar solvents such as methanol, glycol, glycerol, or water; this allowed fluorescence-based viscosity measurements to be performed in these solvent mixtures with readily tunable viscosity. Compound *p*-TPEDMA-1 is obtained by the simple and efficient McMurry reaction of bis[4-(dimethylamino)phenyl]methanone (1). Cross-McMurry coupling between compound 1 and 4-bromobenzophenone (2) offers a TPE derivative (3) as the intermediate for TPE boronic acid (4). Compounds 3 and 4 then undergo Suzuki coupling to give *p*-TPEDMA-2. Compound *p*-TPEDMA-3 is obtained by similar synthetic procedures to those previously described. All compounds were characterized by standard spectroscopic techniques, including ¹H and ¹³C NMR spectroscopy and

HRMS, from which satisfactory analytical data corresponding to the expected chemical structures were obtained (see the Experimental Section and Chart S1 in the Supporting Information).

Aggregation-induced emission (AIE)

UV absorption and normalized photoluminescence (PL) spectra of the precursors in THF and the three target molecules in methanol are shown in Figure S1 and Table S1 in the Supporting Information. Clearly, the protonated compounds possess poorer conjugation than their precursors because the sites of the lone-pair electrons on the dimethylamino (DMA) group are occupied by the protons and have no significant contribution to the molecular conjugation, as revealed by their much bluer absorption and emission. Generally, as the core structure is gradually enlarged, the molar absorptivity gets higher; meanwhile, the absorption and emission signals shift progressively to longer wavelengths. However, the spectrum shift is not very large, especially for TPEDMA molecules, presumably due to their highly twisted conformations. Also, a high-energy emission band is observed at $\lambda \approx 360\text{--}400\text{ nm}$ (Figure 2A, as discussed below, and Figure S3a and S3b in the Supporting Information), which is attributed to the partially photo-oxidized byproduct of TPE-based luminogens.^[18f]

TPE is an archetypical AIE molecule; thus materials constructed from TPE building blocks generally exhibit AIE features. Because TPEDMA molecules are amphiphilic, it is difficult to find appropriate solvent mixtures to demonstrate their AIE features; thus their precursors are used instead. As shown in Figure 1 and Figure S2 in the Supporting Information, *p*-TPEDMA-1, *p*-TPEDMA-2, and *p*-TPEDMA-3 are almost non-emissive in THF due to active intramolecular rotation, which efficiently consumes the energy of the excited state through nonradiative relaxation channels and quenches the emission. Gradual addition of water, which is a poor solvent for luminogens, induces dye molecule aggregate formation and restricts intramolecular rotation. This blocks the nonradiative relaxation channels, and hence, activates the light-emission process. Clearly, all luminogens are AIE-active, and the extent of emission enhancement of *p*-TPEDMA-1, *p*-TPEDMA-2, and *p*-TPEDMA-3 is calculated to be 113, 129, and 173, respectively. The increased number of phenyl ring rotors not only provide more nonradiative channels to consume the excited-state energy, but also improves the quantum efficiency in the aggregated state, at which the RIR process becomes activated and leads to more dramatic fluorescence enhancement.

Viscosity sensitivity

The viscosity response of TPEDMA molecules was first investigated. Steady-state PL spectra of TPEDMA-1, TPEDMA-2, and TPEDMA-3 in mixtures of glycol/glycerol with glycerol volume fractions of 0, 20, 40, 60, and 80%, respectively, were measured and are shown in Figure 2A and Figure S3 in the Supporting Information. As predicted, the fluorescence intensity of the dye molecules is gradually enhanced with increasing solvent

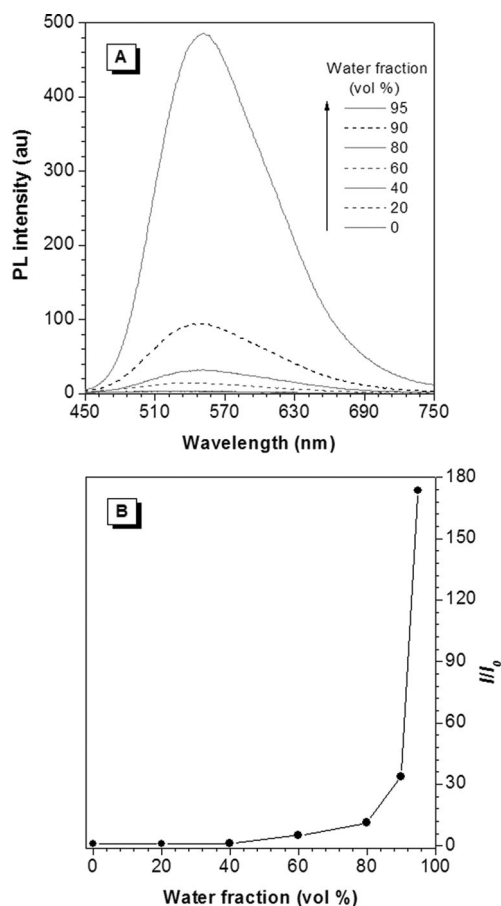


Figure 1. A) PL spectra and B) plots of PL intensity ratio (I/I_0) versus water fraction of *p*-TPEDMA-3 in mixtures of THF/water with different water fractions. I_0 = emission intensity in THF, dye concentration = 10 μM , excitation wavelength = 388 nm.

viscosity without causing a shift in the emission wavelength. According to the AIE mechanism, it is easy to understand that, in more viscous medium, the free volume decreases and the friction between solvent and dye molecules increases. This restricts the intramolecular rotation of the AIE molecules and blocks nonradiative decay; thus enhancing the fluorescence intensity correspondingly.

The curves of $\log I$ versus $\log \eta$ for TPEDMA-1, TPEDMA-2, and TPEDMA-3 are depicted in Figure 2B. All curves can be linearly fitted very well, which indicates that AIE dyes are promising candidates as fluorescent probes to determine bulk solution viscosity. Notably, the corresponding viscosity factors (x) were determined to be 0.46, 0.93, and 0.98, respectively; TPEDMA-2 and TPEDMA-3 were more viscosensitive than molecular rotors (0.4–0.6) and TPA-based rotors (0.57–0.88) reported previously.^[4,7] The value exhibited by TPEDMA-3 (0.98) is the highest viscosity factor, x , reported so far, which is extraordinary. Meanwhile, the viscosity sensitivity of the dye molecules is in the order of TPEDMA-3 > TPEDMA-2 > TPEDMA-1, which illustrates that the addition of more peripheral rotatable phenyl rings results in more sensitive viscosity responses. More nonradiative decay channels are available by increasing the number of rotatable phenyl rings. When they are blocked in

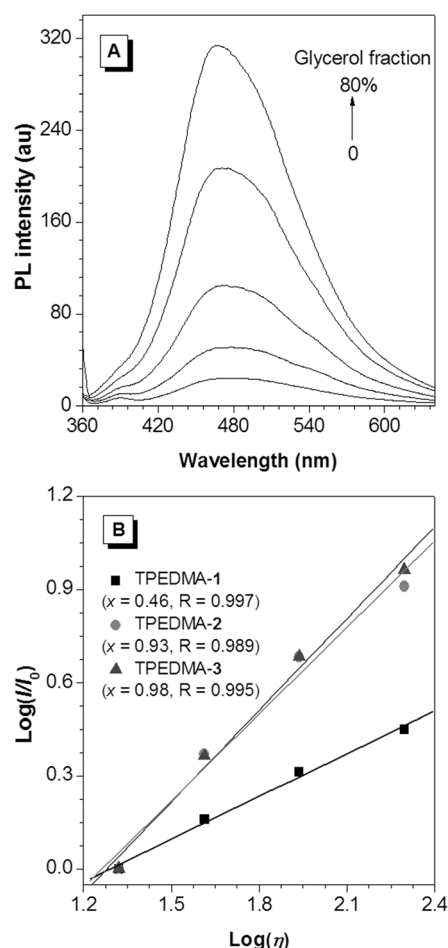


Figure 2. A) PL spectra of TPEDMA-3 in mixtures of glycol/glycerol with glycerol fractions of 0, 20, 40, 60, and 80%. B) Plots of $\log(I/I_0)$ versus $\log \eta$ of TPEDMA-1, TPEDMA-2, and TPEDMA-3; I_0 is the intensity of the solution in glycol, dye concentration = 2 μM , excitation wavelengths: 310 (TPEDMA-1) and 340 nm (TPEDMA-2 and TPEDMA-3).

more viscous medium, more excitons can be populated and undergo radiative decay, and hence, improve the viscosity sensitivity. As described above, the RIR mechanism is the cause of the AIE phenomenon, and rotatable phenyl rings in the AIE molecules can be considered as the ‘executors’ of the RIR mechanism. As viscosity probes, the rotatable phenyl rings in the AIE molecules can also be imagined as the ‘inductors’ of viscosity. Another possibility is that the better conjugation and higher quantum efficiency of TPEDMA-2 and TPEDMA-3 can somehow provide each rotor more room for fluorescence enhancement. Moreover, the enlarged molecular sizes also increase their capability to sense viscosity changes in the surrounding microenvironment owing to greater accessible contact surface areas at the molecular level. The synergy between the increased number of rotors, enhanced quantum efficiency, and enlarged molecular size in TPEDMA-2 and TPEDMA-3 has made their light emission highly sensitive to viscosity changes in the environment and such results provide a promising strategy to design highly viscosensitive AIE dyes.

Figure 3 and Figure S4 in the Supporting Information show the time-resolved fluorescence decay spectra of TPEDMA-1,

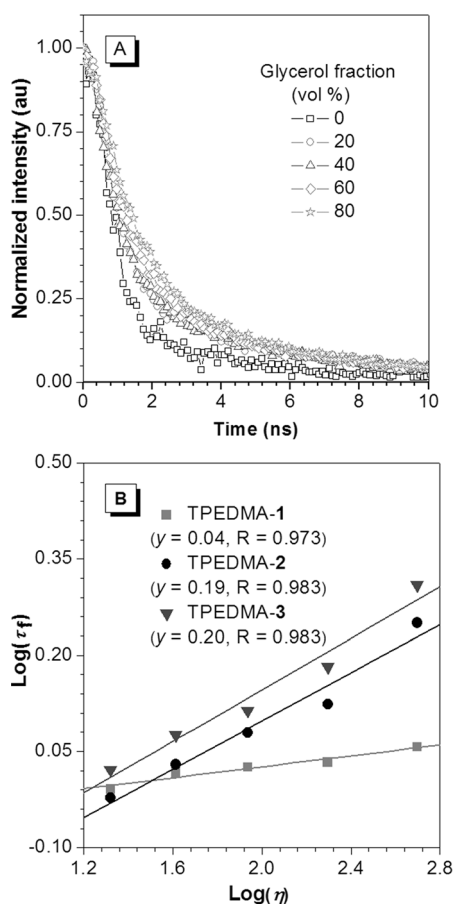


Figure 3. A) Time-resolved fluorescence decay curves of TPEDMA-3 in mixtures of glycol/glycerol with different glycerol volume fractions. B) Plots of $\log \tau_f$ versus $\log \eta$ of TPEDMA molecules. Dye concentration: 2 μM , excitation wavelengths: 310 (TPEDMA-1) and 340 nm (TPEDMA-2 and TPRDMA-3).

TPEDMA-2, and TPEDMA-3 in mixtures of glycol/glycerol with different glycerol volume fractions. Generally, the decay curves point upwards upon increasing the viscosity of the medium, which indicates that the fluorescence lifetime becomes prolonged under such conditions. To gain a further insight into the decay dynamics, the decay parameters obtained by fitting the spectra through a double-exponential function are summarized in Table S2 in the Supporting Information. The excited TPEDMA molecules decay through a fast channel and a negligible slow channel with lifetimes of about 1 and 7–10 ns, respectively. Viscosity can affect the fast decay channel under the employed experimental conditions, and the extent of lifetime enhancement is not as dramatic as that caused by aggregate formation, which can greatly populate the slow decay channels.^[19]

As shown in Figure 3B, all curves exhibit a good linear relationship with calculated viscosity factors of 0.04, 0.19, and 0.20, respectively. Similar to the x values derived from fluorescent intensity, the y values also become larger upon increasing the number of rotatable phenyl rings and the molecular size. Meanwhile, all calculated y values are much smaller than the x values, which shows that the fluorescence lifetime is less viscosensitive than the fluorescence intensity for the AIE sensors.

However, lifetime measurements are more reliable, especially in the presence of various environmental interference factors.^[4] Therefore, there is a balance between sensitivity and reliability when choosing fluorescence methods for viscosity measurements.

Temperature response

It is generally accepted that elevated temperature can quench emission due to thermally activated intramolecular rotations and vibrations.^[2] In particular, in solution, in which AIE-active dye molecules are molecularly dissolved, intramolecular rotations can be greatly facilitated upon heating owing to their flexible conformation. In our previous work, temperature effects were determined to confirm the RIR mechanism for the AIE phenomenon,^[16a] and, herein, the relationship between molecular structures and the temperature response of the AIE molecules was tested according to the above rational design to provide a more detailed understanding of the RIR process.

As shown in Figure 4A and Figure S5 in the Supporting Information, upon gradually increasing the temperature of aqueous solutions of TPEDMA molecules, the PL intensity decreases

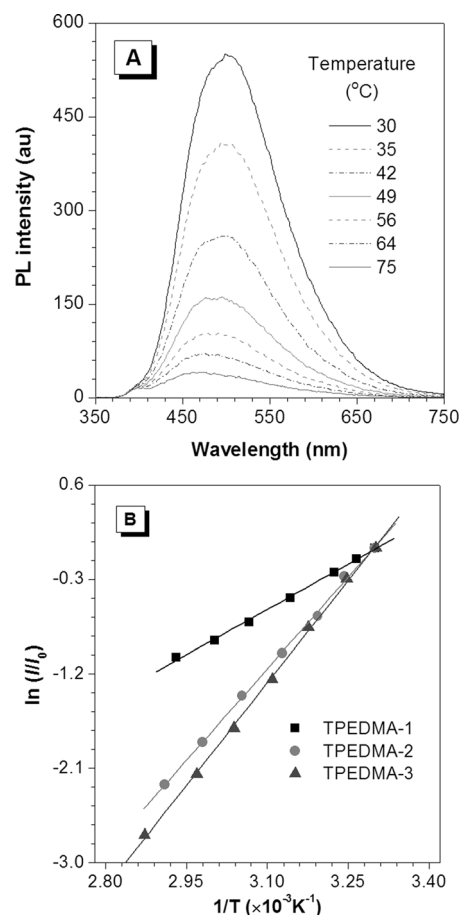


Figure 4. A) PL spectra of TPEDMA-3 in aqueous solution at different temperatures, and B) linear fitting of $\ln(I/I_0)$ versus $1/T$ curves of TPEDMA molecules; I_0 is the intensity of TPEDMA molecules in aqueous solution at 30 °C, dye concentration = 10 μM , excitation wavelengths: 310 (TPEDMA-1) and 340 nm (TPEDMA-2 and TPEDMA-3).

correspondingly, as predicted. Plots of $\ln(I/I_0)$ versus $1/T$ show very good linear relationships ($R^2 > 0.999$), which are indicative of the first-order relationship between I/I_0 and $1/T$, which is the general trend for the effect of temperature on fluorescence.^[2,8b]

A comparative investigation on the temperature response of TPEDMA molecules suggests that TPEDMA-2 and TPEDMA-3, with more rotatable phenyl rings, exhibit more dramatic temperature-quenching effects than that of TPEDMA-1, as shown in Figure 4B. This can be attributed to more channels for nonradiative decay being provided by the larger number of phenyl ring rotors; thus enhancing the temperature sensitivity.

Effective rotors

Either from the viscosity response or temperature effect, we realize that TPEDMA-2 and TPEDMA-3 show much higher sensitivity than that of TPEDMA-1. However, the first two both possess very similar viscosity and temperature responses, although TPEDMA-3 has one more TPE moiety. One may conjecture that, upon increasing the number of rotatable phenyl rings, more intensive intramolecular rotations are accessible to facilitate nonradiative decay; thus improving the viscosity and temperature sensitivity, which are directly related to the RIR mechanism. However, when considering modes that promote nonradiative decay, it is worth bearing in mind that, for a mode to promote internal conversion, it must directly couple to the π -conjugated systems.^[20]

To interpret such ambiguity, theoretical calculations were conducted. The frontier molecular orbitals (MOs) for TPEDMA molecules calculated with DFT at the B3LYP/6-31G(d, p) level by using the Gaussian 09 program are shown in Figure 5. All phenyl rings of TPEDMA-1 and TPEDMA-2 contribute to the HOMO and LUMO, whereas in TPEDMA-3 some peripheral phenyl rings play little role in the conjugation of the molecule

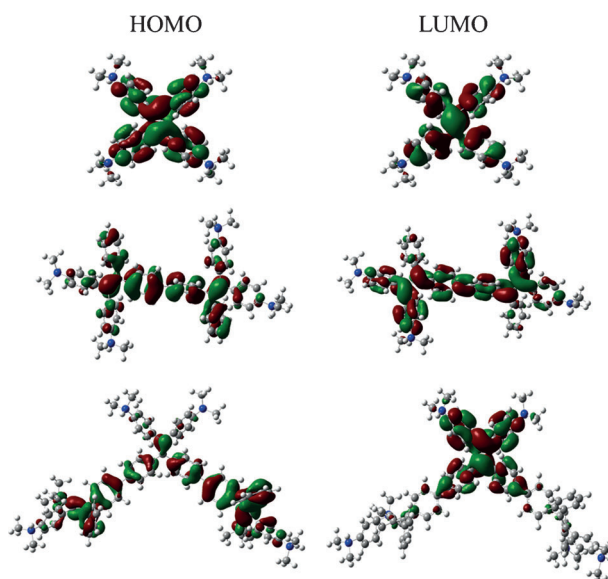


Figure 5. Frontier MOs for TPEDMA molecules calculated with DFT at the B3LYP/6-31G(d, p) level by using the Gaussian 09 program.

due to the highly twisted conformation. Therefore, the number of effective rotatable phenyl rings in TPEDMA-3 is similar to that in TPEDMA-2, although it is clearly much higher than that of TPEDMA-1. This means that, although one more TPE moiety is added to TPEDMA-3, the actual number of rotatable phenyl rings which can effectively promote nonradiative decay only slightly increase, resulting in limited enhancement of the sensitivity response to either viscosity or temperature. Thus, when applying the strategy proposed above to the design of highly sensitive stimuli-responsive probes based on AIE molecules, careful consideration of the effectiveness of the rotors on nonradiative decay of the excited state should be taken.

Meanwhile, the extended π -conjugation framework can significantly increase the excited-state rotation barriers,^[7b] thus reducing the flexibility of the phenyl ring rotors and the sensitivity of the stimuli response, especially in the two-arm-shaped TPEDMA-3. To some extent, this results in only slightly improved sensitivity, even though one more TPE unit is added.

Conclusion

As sensitive and versatile smart materials, AIE luminogens have attracted much interest from mechanistic investigations into materials design. Herein, through rational molecular design, the viscosity and temperature response of AIE rotors can be significantly enhanced with increasing numbers of phenyl ring rotors. For example, AIE rotor TPEDMA-3 exhibits the highest viscosity sensitivity recorded to date, with a viscosity factor of up to 0.98. However, further expansion in the molecular size only results in a limited increase in effective rotors, which is accompanied with increased rotation barriers; thus enhancing the sensitivity only slightly. This molecular design strategy not only offers a feasible route to readily tune the stimuli response of AIE rotors, but also provides a more detailed in-depth understanding of the RIR mechanism.

Experimental Section

General

The synthetic route for TPEDMA molecules is shown in Chart S1 in the Supporting Information. THF (Labscan) was distilled under an atmosphere of dry nitrogen from sodium benzophenone ketyl immediately prior to use. DMF (Labscan) was stirred with calcium hydride overnight, distilled under reduced pressure, and kept under dry nitrogen. Compounds **1**, **2**, and **5**; zinc powder; titanium(IV) chloride; tetrakis(triphenylphosphine)palladium(0); cesium carbonate; and other chemicals were purchased from Aldrich and used as received without further purification. ^1H and ^{13}C NMR spectra were measured on a Bruker ARX 400 NMR spectrometer by using CDCl_3 or $[\text{D}_6]\text{DMSO}$ as deuterated solvents and tetramethylsilane (TMS) as an internal reference. MALDI-TOF spectra were recorded on a GCT Premier CAB048 mass spectrometer operating in chemical ionization (CI) mode with methane as the carrier gas. UV absorption spectra were recorded on a Milton Ray Spectronic 3000 array spectrophotometer. PL spectra were recorded on a PerkinElmer LS 55 spectrofluorometer. Fluorescence decay curves were recorded on an Edinburgh Instruments FLS920 spectrometer combined with

steady-state and time-resolved fluorescence spectrometers. Decay of the PL intensity (I) with time (t) was fitted by a double-exponential function [Eq. (1)] and the weighted mean lifetime, τ , was calculated according to Equation 2,

$$I = A_1 e^{-t/\tau_1} + A_2 e^{-t/\tau_2} \quad (1)$$

$$\langle \tau \rangle = (A_1 \tau_1 + A_2 \tau_2) / (A_1 + A_2) \quad (2)$$

Synthesis

Preparation of *p*-TPEDMA-1: Zinc dust (1.17 g, 18 mmol) and **1** (2.42 g, 9 mmol) were placed into a 150 mL two-necked round-bottomed flask fitted with a reflux condenser. The flask was evacuated under vacuum and purged with dry nitrogen three times. THF (80 mL) was then added. The mixture was cooled to -78°C and TiCl_4 (1 mL, 9 mmol) was slowly added. The mixture was slowly warmed to room temperature, stirred for 0.5 h, and pyridine (0.4 mL, 3.7 mmol) was then injected. After the mixture was heated at reflux overnight, the reaction was quenched with a 10% aqueous solution of K_2CO_3 . A large amount of water was added to the solution until the solid turned gray. The mixture was extracted with dichloromethane three times and the organic layers were combined and washed with brine twice. After evaporation of the solvent under reduced pressure, the crude product was purified by column chromatography on silica gel by using a mixture of ethyl acetate/hexane (1:10, v/v) as the eluent. A yellow solid was obtained in 85% yield. ^1H NMR (400 MHz, $[\text{D}_6]\text{DMSO}$): $\delta = 6.74$ (d, $J = 8.8$ Hz, 8H), 6.43 (d, $J = 9.2$ Hz, 8H), 2.82 ppm (s, 24H); ^{13}C NMR (100 MHz, $[\text{D}_6]\text{DMSO}$): $\delta = 147.8, 132.7, 131.6, 128.5, 111.2, 30.2$ ppm; HRMS (MALDI-TOF): m/z calcd for $\text{C}_{34}\text{H}_{40}\text{N}_4$: 504.3253 $[M^+]$; found: 504.3248; elemental analysis calcd (%) for $\text{C}_{34}\text{H}_{40}\text{N}_4$: C 80.91, H 7.99, N 11.10; found: C 81.05, H 8.04, N 10.91.

Preparation of compound 3: Zinc dust (4.80 g, 74.51 mmol) was placed into a 250 mL two-necked round-bottomed flask equipped with a reflux condenser. The flask was evacuated under vacuum and purged with dry nitrogen three times. Dry THF (100 mL) was then added. The mixture was cooled to -78°C and TiCl_4 (4.2 mL 38.74 mmol) was slowly added. The mixture was slowly warmed to room temperature, stirred for 0.5 h, and heated at reflux for 2 h. Later, pyridine (1.6 mL, 19.37 mmol) was injected. After stirring for 10 min, a solution of **1** (4.00 g, 14.90 mmol) and **2** (5.06 g, 19.38 mmol) in dry THF (40 mL) was injected. Then, the mixture was heated at reflux overnight. The reaction was quenched with a 10% aqueous solution of K_2CO_3 and a large amount of water was added to the solution until the solid turned gray. The mixture was extracted with dichloromethane three times and the organic layers were combined and washed with brine twice. After evaporation of the solvent under reduced pressure, the crude product was purified by column chromatography on silica gel by using a mixture of ethyl acetate/hexane (1:10 v/v) as the eluent. A yellow solid was obtained in 56% yield. ^1H NMR (TMS, 400 MHz, CDCl_3): $\delta = 7.20$ (d, $J = 8.4$ Hz, 2H), 7.12 (m, 3H), 7.05 (m, 2H), 6.90 (m, 6H), 6.48 (m, 4H), 2.89 ppm (d, $J = 10.8$ Hz, 12H); ^{13}C NMR (100 MHz, CDCl_3): $\delta = 148.9, 144.8, 144.3, 141.9, 133.2, 132.52, 132.48, 131.5, 130.7, 127.7, 127.5, 125.7, 119.3, 111.4, 40.4$ ppm; HRMS (MALDI-TOF): m/z calcd for $\text{C}_{30}\text{H}_{29}\text{BrN}_2$: 496.1514 $[M^+]$; found: 496.2000.

Preparation of compound 4: Compound **V3** (3 g, 6 mmol) was placed into a 150 mL two-necked round-bottomed flask. The flask was evacuated under vacuum and purged with dry nitrogen three times. Dry THF (80 mL) was then added. The mixture was cooled to -78°C and 2.5 M *n*BuLi in hexane (3.1 mL 7.84 mmol) was slowly added. After stirring for 1 h, triisopropylborate (4.2 mL,

18.09 mmol) was added in one portion. The mixture was slowly warmed to room temperature and stirred overnight. The reaction was treated with a saturated aqueous solution of ammonium chloride and stirred for 2 h. The mixture was extracted with ethyl acetate three times and the organic layers were combined and washed with brine twice. After evaporation of the solvent under reduced pressure, the crude product was purified by column chromatography on silica gel by using a mixture of ethyl acetate/hexane (1:2, v/v) as the eluent. A yellowish green solid was obtained in 75% yield. ^1H NMR (TMS, 400 MHz, CDCl_3): $\delta = 7.45$ (d, $J = 7.6$ Hz, 2H), 7.09–6.98 (m, 7H), 6.90–6.79 (m, 4H), 6.46 (brs, 4H), 2.88 ppm (s, 12H); ^{13}C NMR spectrum was not obtained due to the poor solubility of the molecule; HRMS (MALDI-TOF): m/z calcd for $\text{C}_{30}\text{H}_{31}\text{BN}_2\text{O}_2$: 462.2479 $[M^+]$; found: 462.4562.

Preparation of *p*-TPEDMA-2: Compound **3** (100 mg, 0.2 mmol), **4** (111 mg, 0.24 mmol), $[\text{Pd}(\text{PPh}_3)_4]$ (12 mg, 0.01 mmol), and C_2CO_3 (195 mg, 0.6 mmol) were placed into a 50 mL two-necked round-bottomed flask equipped with a reflux condenser. The flask was evacuated under vacuum and purged with dry nitrogen three times. DMF (20 mL) was then added. After the mixture was heated at reflux for 24 h, the reaction was quenched with a saturated solution of NH_4Cl , and extracted with dichloromethane three times. The organic layers were combined and washed with brine twice. After evaporation of the solvent under reduced pressure, the crude product was purified by column chromatography on silica gel by using a mixture of ethyl acetate/hexane (1:8 v/v) as the eluent. A yellow solid was obtained in 80% yield. ^1H NMR (TMS, 400 MHz, CDCl_3): $\delta = 7.32$ (d, $J = 8.4$ Hz, 4H), 7.09–7.03 (m, 14H), 6.95–6.89 (m, 8H), 6.50 (brs, 8H), 2.90 ppm (s, 24H); ^{13}C NMR (TMS, 100 MHz, CDCl_3): $\delta = 149.0, 143.6, 140.3, 136.9, 136.5, 132.0, 131.2, 131.0, 128.1, 127.0, 125.1, 111.4, 40.1$ ppm; HRMS (MALDI-TOF): m/z calcd for $\text{C}_{60}\text{H}_{58}\text{N}_4$: 834.4661 $[M^+]$; found: 834.4683; elemental analysis calcd for $\text{C}_{60}\text{H}_{58}\text{N}_4$: C 86.29, H 7.00, N 6.71; found: C 86.39, H 7.11, N 6.50.

Preparation of compound 6: Compound **6** was synthesized according to procedures similar to those used to prepare **3** with **1** and **5** as the starting materials. A yellow powder was obtained in 60% yield. ^1H NMR (TMS, 400 MHz, CDCl_3): $\delta = 7.22$ (d, $J = 8.4$ Hz, 4H), 6.90–6.86 (m, 8H), 6.46 (d, $J = 8.8$ Hz, 4H), 2.92 ppm (s, 12H); ^{13}C NMR (TMS, 100 MHz, CDCl_3): $\delta = 149.0, 143.8, 142.7, 134.0, 133.2, 132.5, 130.8, 127.5, 119.5, 111.3, 40.3$ ppm; HRMS (MALDI-TOF): m/z calcd for $\text{C}_{30}\text{H}_{28}\text{Br}_2\text{N}_2$: 576.3647 $[M^+]$; found: 576.0598.

Preparation of *p*-TPEDMA-3: The synthetic procedure was similar to that used for *p*-TPEDMA-2. A yellowish green solid was obtained in 54% yield. ^1H NMR (TMS, 400 MHz, CDCl_3): $\delta = 7.34$ (d, $J = 8.0$ Hz, 8H), 7.13–7.05 (m, 18H), 6.95–6.89 (m, 12H), 6.50 (brs, 12H), 2.90 ppm (s, 36H); ^{13}C NMR (TMS, 100 MHz, CDCl_3): $\delta = 148.9, 145.2, 144.7, 141.2, 133.3, 132.8, 132.6, 131.92, 131.85, 131.6, 129.2, 127.6, 125.7, 120.5, 113.2, 112.4, 41.3$ ppm; HRMS (MALDI-TOF): m/z calcd for $\text{C}_{90}\text{H}_{86}\text{N}_6$: 1250.6914 $[M^+]$; found: 1251.6964; elemental analysis calcd for $\text{C}_{90}\text{H}_{86}\text{N}_6$: C 86.36, H 6.93, N 6.71; found: C 86.41, H 6.95, N 6.64.

Preparation of aggregates

Stock solutions of *p*-TPEDMA-1, *p*-TPEDMA-2, or *p*-TPEDMA-3 in THF at a concentration of 0.1 mM were prepared. Aliquots (1 mL) of these stock solutions were transferred to 10 mL volumetric flasks. After adding an appropriate amount of THF, water was added dropwise under vigorous stirring to give 10 mM mixtures of THF/water with specific water fractions. The water content was varied in the range of 0–95 vol%. Absorption and emission spectra

of the resulting solutions and aggregates were measured immediately after sample preparation.

Viscosity measurements

The fluorescence-based viscosity measurements were carried out in glycol/glycerol mixtures with glycerol fractions of 0, 20, 40, 60, and 80%. The dye concentration was 2 μM and was four times lower than the typical value (10 μM) for normal PL measurements to ensure that no aggregates formed during measurements. The viscosity of the solvent mixture was also determined by means of a capillary rheometer (Geoffert 2003) for the purposes of comparison. The temperature was kept at 20 °C unless specifically stated otherwise. To prepare the samples, the solvent mixtures (3 mL) with different glycerol volume fractions were thoroughly shaken for 10 min, stock solutions (2 μL , 10^{-3} mol L $^{-1}$) of TPEDMA molecules (prepared with 2 mmol of *p*-TPEDMA molecules in 3 mL of THF with one drop of 37% HCl) were then added followed by further vigorous shaking. So far, various fluorescence-based methods have been used for viscosity measurements, including intensity, ratiometry, lifetime, anisotropy, and fluorescence recovery after photobleaching (FRAP).^[21] Herein, to simplify the investigation on the structure–property relationship, viscosity measurements were carried out based on the change in the PL intensity first. Theoretically, a strict mathematical relationship between viscosity, η , and quantum yield, Φ , existed;^[2] this is known as the Förster–Hoffmann equation [Eq. (3)]:

$$\log \Phi = C + x \log \eta \quad (3)$$

in which C is a temperature-dependent constant and x is a dye-dependent constant that is indicative of the viscosity sensitivity of fluorescence viscosity probes. This relationship was derived analytically and verified experimentally. When we fixed all experimental parameters, including low concentrations (which contributed negligible inner-filter effects), constant temperature, constant absorption, and negligible background light that may affect the intensity in the bulk solution samples under steady-state conditions, the viscosity factor x could be readily derived from Equation (4):

$$x = \log(I_1/I_2) / \log(\eta_1/\eta_2) \quad (4)$$

in which I is the fluorescence intensity.^[22] According to Equation (4), the viscosity factor, x , can be obtained as the slope of the linear fitting of the curve of $\log I$ versus $\log \eta$.

Viscosity measurements based on fluorescence intensity were simple and cheap, but strongly influenced by the dye concentration, fluid optical properties, and other experimental or instrumental factors, especially in complicated in vivo environments. On the contrary, fluorescence lifetime was independent of these factors, which offered an easy calibration process as well as ultrasensitive detection. The quantitative relationship between the fluorescence lifetime (τ_f) and viscosity (η) of the solvent is depicted by the Förster–Hoffmann equation [Eq. (5)]:

$$\log \tau_f = C + y \log \eta \quad (5)$$

in which C is a concentration- and temperature-dependent constant and y is a dye- and temperature-dependent constant, and reflects the viscosity sensitivity of the probes.^[22] It could be readily

derived as the slope from the linear fitting of curves of $\log \tau_f$ versus $\log \eta$.

Temperature effect

To prepare samples for the temperature-effect study, stock solutions (10 μL , 10^{-3} mol L $^{-1}$) of TPEDMA molecules (simply prepared from 2 mmol of *p*-TPEDMA molecules in 3 mL of THF with one drop of 37% HCl) were added to deionized water (3 mL) followed by vigorous shaking. The sample temperature was controlled by means of a circulating water bath, and the exact temperature of the samples was recorded in situ by using a digital thermometer. Generally speaking, fluorescence can be gradually quenched by increasing the temperature, and the fluorescence intensity and temperature follow the modified van 't Hoff equation [Eq. (6)]:^[8b]

$$I/I_0 = Ae^{B/T} \quad (6)$$

Acknowledgements

This work was partially supported by the National Basic Research Program of China (973 Program; 2013CB834701), the Research Grants Council of Hong Kong (604711, 602212, HKUST2/CRF/10, and N_HKUST620/11), the Innovation and Technology Commission (ITCPD/17-9), and the University Grants Committee of Hong Kong (AoE/P-03/08 and T23-713/11-1). B.Z.T. thanks the support from the Guangdong Innovative Research Team Program (201101C0105067115).

Keywords: aggregation · aggregation-induced emission (AIE) · luminescence · structure–activity relationships · synthesis design

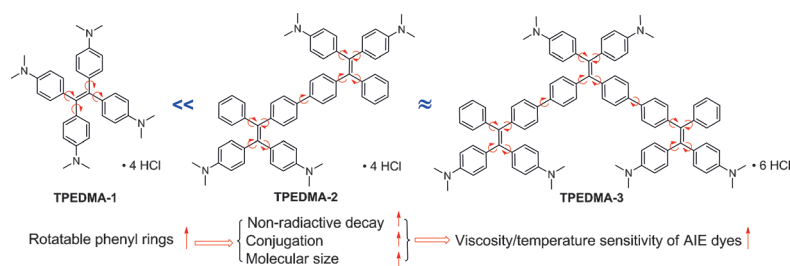
- [1] a) L. Basabe-Desmonts, D. N. Reinhoudt, M. Crego-Calama, *Chem. Soc. Rev.* **2007**, *36*, 993; b) R. Wang, C. Yu, F. Yu, L. Chen, *TrAC Trends Anal. Chem.* **2010**, *29*, 1004; c) N. Boens, W. Qin, M. Baruah, W. M. De Borggraeve, A. Filarowski, N. Smisdom, M. Ameloot, L. Crovetto, E. M. Talavera, J. M. Alvarez-Pez, *Chem. Eur. J.* **2011**, *17*, 10924; d) W. Shi, X. Li, H. Ma, *Angew. Chem. Int. Ed.* **2012**, *51*, 6432; *Angew. Chem.* **2012**, *124*, 6538; e) K. Zhou, H. Liu, S. Zhang, X. Huang, Y. Wang, G. Huang, B. D. Sumer, J. Gao, *J. Am. Chem. Soc.* **2012**, *134*, 7803; f) M. J. Marín, F. Galindo, P. Thomas, D. A. Russell, *Angew. Chem. Int. Ed.* **2012**, *51*, 9657; *Angew. Chem.* **2012**, *124*, 9795.
- [2] a) G. Liebsch, I. Klimant, O. S. Wolfbeis, *Adv. Mater.* **1999**, *11*, 1296; b) A. Mills, C. Tommons, R. T. Bailey, M. C. Tedford, P. J. Crilly, *Analyst* **2006**, *131*, 495; c) F. H. C. Wong, D. S. Banks, A. Abu-Arish, C. Fradin, *J. Am. Chem. Soc.* **2007**, *129*, 10302; d) X. Xiao, Y. Fu, J. Zhou, Z. Bo, L. Li, C. M. Chan, *Macromol. Rapid Commun.* **2007**, *28*, 1003; e) A. S. Kocincova, S. M. Borisov, C. Krause, O. S. Wolfbeis, *Anal. Chem.* **2007**, *79*, 8486; f) N. Tian, A. Thiessen, R. Schiewek, O. J. Schmitz, D. Hertel, K. Meerholz, E. Holder, *J. Org. Chem.* **2009**, *74*, 2718; g) C. D. S. Brites, P. P. Lima, N. J. O. Silva, A. Millán, V. S. Amaral, F. Palacio, L. D. Carlos, *Adv. Mater.* **2010**, *22*, 4499.
- [3] a) J. Kavandi, J. Callis, M. Gouterman, G. Khalil, D. Wright, E. Green, D. Burns, B. McLachlan, *Rev. Sci. Instrum.* **1990**, *61*, 3340; b) W. Xu, R. C. McDonough, B. Langsdorf, J. N. Demas, B. A. DeGraff, *Anal. Chem.* **1994**, *66*, 4133; c) B. G. McLachlan, J. H. Bell, *Exp. Therm. Fluid Sci.* **1995**, *10*, 470; d) M. Gouterman, *J. Chem. Educ.* **1997**, *74*, 697; e) T. Liu, M. Guille, J. P. Sullivan, *AIAA J.* **2001**, *39*, 103; f) J. W. Gregory, A. Asai, M. Kamada, T. Liu, J. P. Sullivan, *Proc. Inst. Mech. Eng. G J. Aerospace Eng.* **2008**, *222*, 249.
- [4] a) K. L. Luby-Phelps, S. Mujumdar, R. B. Mujumdar, L. A. Ernst, W. Galbraith, A. S. Waggoner, *Biophys. J.* **1993**, *65*, 236; b) K. Suhling, P. M. W. French, D. Phillips, *Photochem. Photobiol. Sci.* **2005**, *4*, 13; c) M. A. Hai-

- dekker, T. P. Brady, D. Lichlyter, E. A. Theodorakis, *J. Am. Chem. Soc.* **2006**, *128*, 398; d) D. E. Fischer, E. A. Theodorakis, M. A. Haidekker, *Nat. Protoc.* **2007**, *2*, 227; e) M. K. Kuimova, G. Yahioğlu, J. A. Levitt, K. Suhlring, *J. Am. Chem. Soc.* **2008**, *130*, 6672; f) M. K. Kuimova, S. W. Botchway, A. W. Parker, M. Balaz, H. A. Collins, H. L. Anderson, K. Suhlring, P. R. Ogilby, *Nat. Chem.* **2009**, *1*, 69; g) J. A. Levitt, M. K. Kuimova, G. Yahioğlu, P. H. Chung, K. Suhlring, D. Phillip, *J. Phys. Chem. C* **2009**, *113*, 11634; h) X. Peng, Z. Yang, J. Wang, J. Fan, Y. He, F. Song, B. Wang, S. Sun, J. Qu, J. Qi, M. Yan, *J. Am. Chem. Soc.* **2011**, *133*, 6626.
- [5] a) Y. Sagara, T. Kato, *Angew. Chem.* **2008**, *120*, 5253; b) Y. Sagara, T. Kato, *Nat. Chem.* **2009**, *1*, 605; c) A. Pucci, G. Ruggeri, *J. Mater. Chem.* **2011**, *21*, 8282; d) A. Pucci, R. Bizzaricc, G. Ruggeri, *Soft Mater.* **2011**, *7*, 3689; e) K. Ariga, T. Mori, J. P. Hill, *Adv. Mater.* **2012**, *24*, 158; f) Z. Chi, X. Zhang, B. Xu, X. Zhou, C. Ma, Y. Zhang, S. Liu, J. Xu, *Chem. Soc. Rev.* **2012**, *41*, 3878.
- [6] a) M. V. Alfimov, O. A. Fedorova, S. P. Gromov, *J. Photochem. Photobiol. A* **2003**, *158*, 183; b) L. Zhu, W. Wu, M. Zhu, J. J. Han, J. K. Hurst, A. D. Q. Li, *J. Am. Chem. Soc.* **2007**, *129*, 3524; c) J. Fölling, V. Belov, R. Kunetsky, R. Medda, A. Schonle, A. Egner, C. Eggeling, M. Bossi, S. W. Hell, *Angew. Chem. Int. Ed.* **2007**, *46*, 6266; d) Z. Hu, Q. Zhang, M. Xue, Q. Sheng, Y. G. Liu, *Opt. Mater.* **2008**, *30*, 851; e) Z. Tian, W. Wu, A. D. Q. Li, *ChemPhysChem* **2009**, *10*, 2577; f) H. L. Wong, W. T. Wong, V. W. W. Yam, *Org. Lett.* **2012**, *14*, 1862.
- [7] a) J. Sutharsan, D. Lichlyter, N. E. Wright, M. Dakanali, M. A. Haidekker, E. A. Theodorakis, *Tetrahedron* **2010**, *66*, 2582; b) F. Zhou, J. Shao, Y. Yang, J. Zhao, H. Guo, X. Li, S. Ji, Z. Zhang, *Eur. J. Org. Chem.* **2011**, *2011*, 4773.
- [8] a) A. Malliaris, J. L. Moigne, J. Sturm, R. Zana, *J. Phys. Chem.* **1985**, *89*, 2709; b) N. Chandrasekharan, L. A. Kelly, *J. Am. Chem. Soc.* **2001**, *123*, 9898.
- [9] a) C. Li, Y. Zhang, J. Hu, J. Cheng, S. Liu, *Angew. Chem. Int. Ed.* **2010**, *49*, 5120; *Angew. Chem.* **2010**, *122*, 5246; b) J. Chen, P. Zhang, G. Fang, P. Yi, F. Zeng, S. Wu, *J. Phys. Chem. B* **2012**, *116*, 4354.
- [10] J. Feng, K. Tian, D. Hu, S. Wang, S. Li, Y. Zeng, Y. Li, G. Yang, *Angew. Chem. Int. Ed.* **2011**, *50*, 8072; *Angew. Chem.* **2011**, *123*, 8222.
- [11] J. Zhang, A. Peng, H. Fu, Y. Ma, T. Zhai, J. Yao, *J. Phys. Chem. A* **2006**, *110*, 9079.
- [12] a) J. B. Birks, *Photophysics of Aromatic Molecules*, Wiley, New York, **1970**; b) N. J. Turro, V. Ramamurthy, J. C. Scaiano, *Modern Molecular Photochemistry of Organic Molecules*, University Science Books, Sausalito, **2010**.
- [13] a) Y. Hong, J. W. Y. Lam, B. Z. Tang, *Chem. Commun.* **2009**, 4332; b) Y. Hong, J. W. Y. Lam, B. Z. Tang, *Chem. Soc. Rev.* **2011**, *40*, 5361; c) A. Qin, J. W. Y. Lam, B. Z. Tang, *Prog. Polym. Sci.* **2012**, *37*, 182; d) D. Ding, K. Li, B. Liu, B. Z. Tang, *Acc. Chem. Res.* **2013**, *46*, 2441.
- [14] a) Y. Dong, J. W. Y. Lam, A. Qin, Z. Li, J. Liu, J. Sun, Y. Dong, B. Z. Tang, *Chem. Phys. Lett.* **2007**, *446*, 124; b) S. Chen, J. Liu, Y. Liu, H. Su, Y. Hong, C. K. W. Jim, R. T. K. Kwok, N. Zhao, W. Qin, J. W. Y. Lam, K. S. Wong, B. Z. Tang, *Chem. Sci.* **2012**, *3*, 1804; c) S. Chen, Y. Hong, Y. Liu, J. Liu, C. W. T. Leung, M. Li, R. T. K. Kwok, E. Zhao, J. W. Y. Lam, Y. Yu, B. Z. Tang, *J. Am. Chem. Soc.* **2013**, *135*, 4926; d) Z. Yang, W. Qin, J. W. Y. Lam, S. Chen, H. H. Y. Sung, I. D. Williams, B. Z. Tang, *Chem. Sci.* **2013**, *4*, 3725.
- [15] a) J. W. Chung, B. K. An, S. Y. Park, *Chem. Mater.* **2008**, *20*, 6750; b) L. Tang, J. K. Jin, A. Qin, W. Z. Yuan, Y. Mao, J. Mei, J. Z. Sun, B. Z. Tang, *Chem. Commun.* **2009**, 4974; c) C. T. Lai, R. H. Chien, S. W. Kuo, J. L. Hong, *Macromolecules* **2011**, *44*, 6546.
- [16] a) J. Chen, W. C. C. Law, J. W. Y. Lam, Y. Dong, S. M. F. Lo, I. D. Williams, D. B. Zhu, B. Z. Tang, *Chem. Mater.* **2003**, *15*, 1535; b) R. Hu, E. Lager, A. Aguilar-Aguilar, J. Liu, J. W. Y. Lam, H. H. Y. Sung, I. D. Williams, Y. Zhong, K. S. Wong, E. Pena-Cabrera, B. Z. Tang, *J. Phys. Chem. C* **2009**, *113*, 15845.
- [17] a) X. Luo, J. Li, C. Li, L. Heng, Y. Q. Dong, Z. Liu, Z. Bo, B. Z. Tang, *Adv. Mater.* **2011**, *23*, 3261; b) J. Mei, J. Wang, A. Qin, H. Zhao, W. Yuan, Z. Zhao, H. H. Y. Sung, C. Deng, S. Zhang, I. D. Williams, J. Z. Sun, B. Z. Tang, *J. Mater. Chem.* **2012**, *22*, 4290; c) N. Zhao, Y. Zhang, J. W. Y. Lam, H. H. Y. Sung, N. Xie, S. Chen, H. Su, M. Gao, I. D. Williams, K. S. Wong, B. Z. Tang, *Chem. Commun.* **2012**, *48*, 8637; d) W. Yuan, Y. Tan, Y. Gong, P. Lu, J. W. Y. Lam, X. Shen, C. Feng, H. H. Y. Sung, Y. Lu, I. D. Williams, J. Z. Sun, Y. Zhang, B. Z. Tang, *Adv. Mater.* **2013**, *25*, 2837.
- [18] a) Z. Li, Y. Dong, B. X. Mi, Y. H. Tang, M. Haussler, H. Tong, Y. P. Dong, J. W. Y. Lam, Y. Ren, H. H. Y. Sung, K. S. Wong, P. Gao, I. D. Williams, H. S. Kwok, B. Z. Tang, *J. Phys. Chem. B* **2005**, *109*, 10061; b) H. Tong, Y. Q. Dong, Y. N. Hong, M. Haussler, J. W. Y. Lam, H. H. Y. Sung, X. M. Yu, J. X. Sun, I. D. Williams, H. S. Kwok, B. Z. Tang, *J. Phys. Chem. C* **2007**, *111*, 2287; c) A. Qin, J. W. Y. Lam, F. Mahtab, C. K. W. Jim, L. Tang, J. Z. Sun, H. H. Y. Sung, I. D. Williams, B. Z. Tang, *Appl. Phys. Lett.* **2009**, *94*, 253308; d) Z. Zhao, J. W. Y. Lam, C. Y. K. Chan, S. Chen, J. Liu, P. Lu, M. Rodriguez, J. L. Maldonado, G. Ramos-Ortiz, H. H. Y. Sung, I. D. Williams, H. Su, K. S. Wong, Y. Ma, H. S. Kwok, H. Qiu, B. Z. Tang, *Adv. Mater.* **2011**, *23*, 5430; e) J. Shi, N. Chang, C. Li, J. Mei, C. Deng, X. Luo, Z. Liu, Z. Bo, Y. Q. Dong, B. Z. Tang, *Chem. Commun.* **2012**, *48*, 10675; f) P. M. Aldred, C. Li, M.-Q. Zhu, *Chem. Eur. J.* **2012**, *18*, 16037.
- [19] a) M. H. Lee, D. Kim, J. W. Y. Lam, B. Z. Tang, *J. Korean Phys. Soc.* **2004**, *45*, 329; b) Y. Ren, J. W. Y. Lam, Y. Dong, B. Z. Tang, K. S. Wong, *J. Phys. Chem. B* **2005**, *109*, 1135; c) Y. Ren, Y. Dong, J. W. Y. Lam, B. Z. Tang, K. S. Wong, *Chem. Phys. Lett.* **2005**, *402*, 468; d) C. J. Bhongale, C. W. Chang, E. W. G. Diau, C. S. Hsu, Y. Dong, B. Z. Tang, *Chem. Phys. Lett.* **2006**, *419*, 444.
- [20] a) J. S. Wilson, N. Chawdhury, M. R. A. Al-Mandhary, M. Younus, M. S. Khan, P. R. Raithby, A. Köhler, R. H. Friend, *J. Am. Chem. Soc.* **2001**, *123*, 9412; b) J. S. Wilson, R. J. Wilson, R. H. Friend, A. Köhler, M. K. Al-Suti, M. R. A. Al-Mandhary, M. S. Khan, *Phys. Rev. B* **2003**, *67*, 125206; c) A. Köhler, H. Bässler, *Mater. Sci. Eng. R* **2009**, *66*, 71.
- [21] M. A. Haidekker, E. A. Theodorakis, *Org. Biomol. Chem.* **2007**, *5*, 1669.
- [22] a) Th. Förster, G. Hoffmann, *Z. Phys. Chem.* **1971**, *75*, 63; b) R. O. Loutfy, *Pure Appl. Chem.* **1986**, *58*, 1239; c) C. E. Kung, J. K. Reed, *Biochemistry* **1986**, *25*, 6114; d) T. Iwaki, C. Torioe, M. Noji, M. Nakanishi, *Biochemistry* **1993**, *32*, 7589; e) M. A. Haidekker, J. A. Frangos, *Proc. Soc. Photo-Opt. Instrum. Eng.* **2000**, 3921, 101.

Received: September 3, 2014

Published online on ■■■■■, 0000

FULL PAPER




On demand: A new molecular design strategy to rationally tune the stimuli response of luminescent materials with aggregation-induced emission (AIE) characteristics has been developed. Increasing the number of rotatable

phenyl rings enhances the sensitivity of the response of AIE rotors to viscosity and temperature until higher rotational barriers prevent further enhancement (see scheme).

Structure–Activity Relationships

J. Li, Y. Zhang, J. Mei, J. W. Y. Lam, J. Hao, B. Z. Tang*



Aggregation-Induced Emission Rotors: 
Rational Design and Tunable Stimuli Response